

Topology-induced confined superfluidity in inhomogeneous arrays

P. Buonsante,¹ R. Burioni,² D. Cassi,² V. Penna,¹ and A. Vezzani²

¹*Dipartimento di Fisica, Politecnico di Torino and I.N.F.M.,
Corso Duca degli Abruzzi 24 - I-10129 Torino (ITALIA)*

²*Dipartimento di Fisica, Università degli Studi di Parma and I.N.F.M.,
Parco Area delle Scienze 7/a I-43100 Parma (ITALIA)*

(Dated: March 22, 2002)

We report the first study of the zero-temperature phase diagram of the Bose-Hubbard model on topologically inhomogeneous arrays. We show that the usual Mott-insulator and superfluid domains, in the paradigmatic case of the comb lattice, are separated by regions where the superfluid behaviour of the bosonic system is confined along the comb backbone. The existence of such *confined superfluidity*, arising from topological inhomogeneity, is proved by different analytical and numerical techniques which we extend to the case of inhomogeneous arrays. We also discuss the relevance of our results to real system exhibiting macroscopic phase coherence, such as coupled Bose condensates and Josephson arrays.

PACS numbers: 05.30.Jp, 73.43.Nq, 74.81.Fa, 03.75.Lm

I. INTRODUCTION

The Bose-Hubbard (BH) Hamiltonian, describing bosons hopping across the sites of a discrete structure and originally introduced to model liquid He in confined geometries,¹ proves successful in capturing the essential physics of a wide range of condensed-matter systems. The best known examples are no doubt provided by Josephson-junction arrays (JJA)^{2,3} and Bose-Einstein condensate (BEC) arrays,^{4,5} which are the subject of a huge amount of both theoretical and experimental ongoing investigations. The hallmark of such class of systems is the presence of a superfluid phase as opposed to a (Mott) insulator phase.⁶ The theoretical studies hitherto carried out on such phase transition mostly focus on homogeneous ambient lattices, and provide well-established numerical and analytical techniques. Homogeneous lattices are also the basis of the current experimental realizations of systems belonging to the BH class. This is at least partly due to present technical constraints. For instance the optical techniques used to fragment BECs yield quite naturally homogeneous arrays.

However, the striking progress in experimental techniques suggests the realization of inhomogeneous networks to be at hand. Actually, JJAs can be engineered in nontrivial geometries with the only possible constraint of planarity. In this respect, interesting geometry-driven effects are proposed in Refs. 7,8, while the physics of a fractal JJA is experimentally studied in Ref. 9. As to BEC arrays, two very promising approaches for realizing inhomogeneous topologies are provided by holographic optical traps^{10,11} and magnetic microtraps^{12,13,14}. In the latter case, ongoing efforts are aimed at reducing the spacing between individual microtraps, currently bound above a few μm , in order to couple the condensates therein confined.

The deep influence of topological inhomogeneities on thermodynamic properties of discrete boson systems is evidenced by the occurrence of unexpected features even

in the absence of boson interaction. Indeed, a finite-temperature Bose-Einstein condensation can take place despite the low dimensionality of the system. This is illustrated in Refs. 15,16 in the case of the square comb lattice, namely an array of linear chains (fingers) joined along a transverse direction (backbone) such as the one shown in the inset of Fig. 1. More precisely, inhomogeneity induces a *hidden* band in the single-particle energy spectrum which is ultimately responsible for condensation.

On the other hand, the rich zero-temperature phase diagram of the BH model ensues from the competition between the on-site repulsion and the kinetic energy of the boson gas. In the light of this, a natural question arises as to the influence of topology on the physics of interacting bosons. In this respect we mention that the effect of the inhomogeneity arising from the superposition of a local on-site potential on an otherwise regular lattice has been recently addressed. In particular, the existence of local Mott domains induced by a parabolic confining potential has been evidenced for BEC arrays in Refs. 17, 18,19,20,21 while Refs. 22,23,24,25 analyze the phase diagram on superlattices.

Here, we consider inhomogeneities of purely topological (i.e. kinetic rather than potential) origin, focusing on the emblematic case of comb lattices, where the larger connectivity of the backbone is expected to act as a catalyst for superfluidity. Interestingly, the competition between kinetic and boson-interaction energy causes the occurrence of an intermediate domain in the BH phase diagram. The usual Mott-insulator lobes are separated from the superfluid domain by a phase characterized by the localization of superfluidity in a narrow region surrounding the comb backbone, the rest of the structure exhibiting an unexpected insulator-like behavior. More precisely, we show that the *local compressibility*¹⁹ features an exponential decrease with increasing distance from the backbone. Note indeed that the topological inhomogeneity of the structure requires a description in terms

of site-dependent quantities. These results, which — to the best of our knowledge — are the first concerning the influence of topology on the BH phase diagram, required the generalization of different numerical and analytical techniques²⁶. The presence of *confined superfluidity* is first evidenced within a mean-field approach, and further confirmed by both a third order analytical strong coupling perturbative expansion (SCPE) and (population) quantum Monte-Carlo (QMC) simulations.

II. THE BOSE-HUBBARD MODEL ON A GENERIC STRUCTURE

The BH Hamiltonian, describing locally interacting bosons on a generic discrete structure consisting of M sites, is

$$H = \sum_{j=1}^M \left[\frac{U}{2} n_j(n_j - 1) - \mu n_j \right] - T \sum_{h,j=1}^M A_{hj} a_h a_j^\dagger \quad (1)$$

where the operator a_j^\dagger (a_j) creates (annihilates) a boson at site j and $n_j = a_j^\dagger a_j$ counts the bosons sitting at site j . As to the parameters, $U > 0$ accounts for the (on-site) repulsion among bosons, μ is the chemical potential and T is the hopping amplitude between adjacent sites, specified by the adjacency matrix A . This is a useful tool supplied by graph theory,²⁷ allowing an algebraic description of the topology of a generic discrete structure. Its generic matrix element A_{hj} is one if sites (h, j) are nearest neighbors and zero otherwise. In view of $[N, H] = 0$, where $N = \sum_j n_j$, Hamiltonian (1) can be conveniently studied exploiting its block-diagonal structure. Since we are interested in the zero temperature phase diagram, hereafter $\langle \cdot \rangle$ denotes the expectation value on the ground state of H .

As we mentioned above, in the case of homogeneous topology the competition between on-site interaction and hopping gives rise to an interesting zero-temperature phase-diagram in the μ/U - T/U plane, where two different domains can be recognized. A superfluid phase, where the energy cost of adding or subtracting a boson to the system vanishes in the thermodynamic limit; An incompressible Mott-insulator phase, consisting of a series of adjacent lobes, where such operations cost a finite amount of energy and the filling $f \equiv N/M$ is pinned to an integer value. The Mott-superfluid transition can be furthermore characterized by the compressibility $\kappa = \partial N / \partial \mu$, which is finite in the superfluid region and vanishes within the Mott lobes. In the case of inhomogeneous systems, the possible effects of topology can be described in detail by the site-dependent *local compressibility*,¹⁹ $\kappa_j = \partial \rho_j / \partial \mu$, where $\rho_j = \langle n_j \rangle$ is the local density of bosons.

Owing to the enormous size of the Fock space, an exact solution of the model cannot be faced even for relatively small structures. However, the essential elements of the Mott-superfluid transition can be captured

resorting to different approximate schemes, such as mean-field,^{28,29} SCPE,³⁰ the renormalization approach³¹ and QMC computations.^{32,33}

III. MEAN-FIELD APPROXIMATION

The key point of the mean-field approach of Ref. 28 consists in the approximation

$$(a_h - \langle a_h \rangle) (a_j^\dagger - \langle a_j^\dagger \rangle) \approx 0 \quad (2)$$

allowing to recast Hamiltonian (1) as the sum of on-site Hamiltonians $H \approx \mathcal{H} = \sum_j \mathcal{H}_j$. In the simple case of a d -dimensional (translationally invariant) lattice, \mathcal{H}_j is site independent and one is left with a single site problem²⁸

$$\mathcal{H}(\alpha) = M \left[\frac{U}{2} n(n-1) - \mu n - 2dT(a + a^\dagger)\alpha + 2dT\alpha^2 \right],$$

subject to the self consistency constraint $\alpha = \langle a \rangle$,³⁴ where the so-called *superfluid parameter* α can be considered real without loss of generality. The phase diagram of the homogeneous case can be obtained numerically²⁸ or even analytically.^{25,35}

For non-homogeneous structures

$$\mathcal{H}(\{\alpha_h\}) = \sum_{j=1}^M \mathcal{H}_j \quad (3)$$

$$\begin{aligned} \mathcal{H}_j &= \frac{U}{2} n_j(n_j - 1) - \mu n_j \\ &- T \sum_{h=1}^M A_{jh} \alpha_h (a_j + a_j^\dagger - \alpha_j) \end{aligned} \quad (4)$$

and the ground state of \mathcal{H} has the form $|\psi\rangle = \bigotimes_j |j; \{\alpha_h\}\rangle$, where $|j; \{\alpha_h\}\rangle$ is the ground state of \mathcal{H}_j . Thus the problem is solved by finding the set of real quantities $\{\alpha_h\}_{h=1}^M$ such that

$$\langle j; \{\alpha_h\} | a_j | j; \{\alpha_h\} \rangle = \alpha_j. \quad (5)$$

This can be easily done numerically by means of self-consistent iterative algorithm.^{17,25} Despite the approximation in Eq. (2) strongly suppresses spatial correlation, some topological information is retained in the above mean-field formulation owing to the presence of the adjacency matrix A in Hamiltonian (3). In this case ρ_j , k_j and α_j are in general site-dependent quantities. For comb lattices these quantities are constant along the backbone direction, owing to the symmetry of the system.

Fig. 1 shows the numerically determined mean-field phase diagram for a 100×100 comb lattice. In the regions I_f (where f is the integer filling) $\kappa_j = 0$ for all j 's and the total number of bosons is pinned at $N = fM$. The system is therefore an incompressible Mott insulator. In the regions II_f , κ_j is finite, yet it vanishes exponentially along the fingers. The same behaviour is observed for ρ_j , which is exponentially close to f with increasing distance

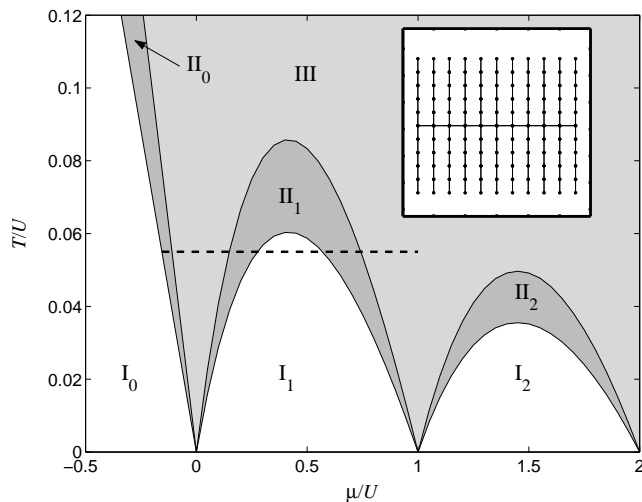


FIG. 1: **Inset:** an example of square comb lattice featuring 11 sites both on the backbone and on the ribs³⁶; **Main plot:** Mean-field Phase diagram of a 100×100 comb lattice. Different shades of grey denote different phases. The dashed line at $T/U = 0.055$ signals the set of parameters considered in Fig. 2.

from the backbone. Hence in these regions the superfluid behaviour of the system is confined along the backbone direction alone. An extended superfluid behaviour is recovered in region III, where the local density ρ_j far from the backbone is not necessarily an integer quantity, and κ_j is nowhere vanishing. Such behaviour of the local density of bosons and compressibility are summarized in Fig. 2 and in the upper panel of Fig. 3, respectively.

We mention that it is possible to evaluate the exact analytical form of the boundaries of the I_f regions as provided by the mean-field approach described by Eqs. (3)–(5). This can be for instance accomplished making use of the finite-temperature method reported in Ref. 25, and subsequently letting the temperature go to zero. The function of T/U describing the I_f boundary for a generic structure characterized by the adjacency matrix A is obtained by rescaling the corresponding function for a homogeneous d -dimensional lattice^{25,35} by a factor $\frac{\lambda}{2d}$, where λ is the maximal eigenvalue of A .

In general, topological inhomogeneities make the study of critical behaviours a rather difficult task. However, the above results suggest some considerations in this respect. On regular lattices the correlation length diverges in any direction at a critical point. Conversely, on the comb lattice, the correlation length is expected to diverge only along a specific direction, depending on the critical border under concern. To wit, the correlation length between sites of the same finger is the only divergent quantity at the II_f –III transition, while it is finite at the border between regions I_f and II_f (where the divergent quantity is the correlation length between sites of different fingers). We also mention that preliminary re-

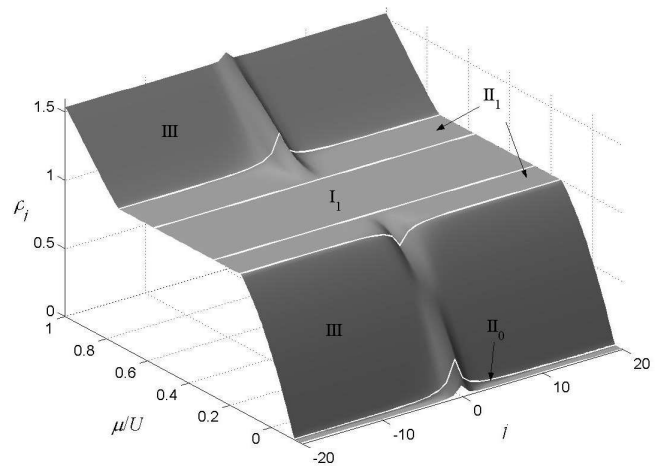


FIG. 2: Behaviour of the local density of bosons ρ_j for sites j along a finger of the comb lattice ($j = 0$ backbone). The figure refers to a fixed value of the hopping amplitude $T/U = 0.055$ and a finite interval of μ/U (dashed line in Fig. 1). The white density profiles correspond to the borders of the different regions of the phase diagram. As we discussed in the text $\rho_j = 1$ inside region I_1 , $\rho_j \rightarrow f$ in regions II_f , whereas ρ_j tends to a not necessarily integer number in region III.

sults based on the mean-field approach of Ref. 25 indicate that the above picture is robust at small finite temperatures, and hence in principle accessible to experiments. In this respect we note that the three different phases in Fig. 1 can be probed as in Ref. 5, provided that the system is realized in terms of coupled BECs, possibly using holographic traps.^{10,11} Indeed, after the trapping potential is released, the expanding atomic clouds should produce either a one-dimensional³⁷ or a two-dimensional³⁸ interference pattern depending on whether superfluidity is confined along the backbone or extended on the entire comb.

IV. BEYOND MEAN-FIELD

A step beyond the mean-field approximation consists in the strong coupling perturbative expansion. Indeed, time-independent perturbation theory in the hopping parameter allows to obtain an analytical approximation of the Mott lobes, which, in the case of the linear chain, proves to be quite satisfactory already at the third order.³⁰ This approach, introduced in Ref. 30 for homogeneous bipartite structures, is extended to any structure in Ref. 26. Quite interestingly, it turns out that topological inhomogeneity gives rise to a third-order correction featuring an unusual dependence on the adjacency matrix describing the topology of the structure. Indeed, unlike the previously reported perturbative terms, depending only on the maximal eigenpair of A , the “topological correction” depends on the entire spectrum of the adjacency matrix. The solid line in the inset of Fig. 4 is the border of

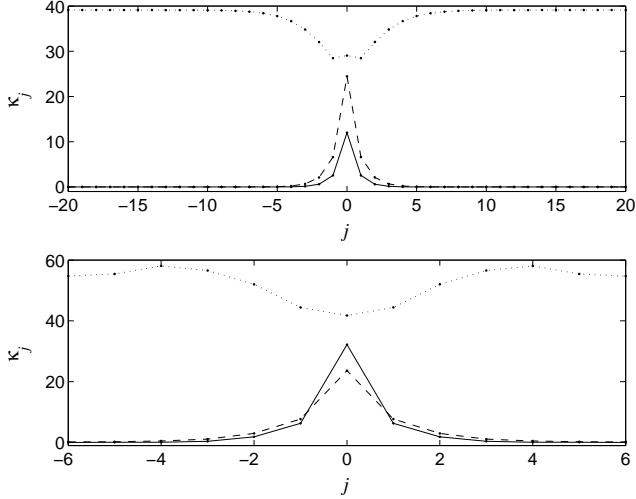


FIG. 3: Local compressibility κ_j for sites j along one finger of the comb lattice ($j = 0$ is on the backbone). Dashed, solid and dotted lines refer to region II_0 , II_1 and III , respectively. Note the exponential decrease with increasing distance from the backbone characterizing the first two curves. **Upper panel:** Mean-field result. **Lower panel:** QMC data for a 12×12 lattice.

the Mott lobe I_1 for a comb lattice as provided by the analytical third-order strong-coupling perturbative expansion reported in Ref. 26. The above described exponential localization of superfluidity characterizing phases II_f is also captured by SCPE even at order zero. Indeed it can be easily shown that $\rho_j = f + C|v_j|^2$ and $\kappa_j = K|v_j|^2$, where C and K are normalizing constants and v_j is the j -th component of the maximal eigenvector of the adjacency matrix, depending only on the distance d_j from the backbone,^{15,16} $v_j = \exp[-d_j \text{asinh}(1)]$. First order SCPE confirms this behaviour, though with a different decay rate, as well as the above considerations about the correlation functions.²⁶

The data points in the inset of Fig. 4, satisfactorily agreeing with the perturbative curve, have been obtained with a population QMC approach³⁹ adopting the resampling procedure described in Ref. 40. Based on a generalization of the power method for finding the maximal eigenpair of a matrix, this technique essentially amounts to a stochastic evaluation of the ground state of Hamiltonian (1) and therefore allows to study the zero temperature phase diagram of the BH model. Note that both in the SCPE and in the QMC approach μ is evaluated as the difference between the ground state energies of systems whose total number of bosons differs by one.^{30,32} In particular, the border of phases I_f are obtained considering the energy cost of adding or subtracting one boson from the integer filling situation $N = Mf$.

The QMC approach also confirms the existence of the confined superfluid phases II_f . Fig. 4 clearly shows the transition between phases II_0 and III . Indeed in the former region the local density ρ_j at a site far from the back-

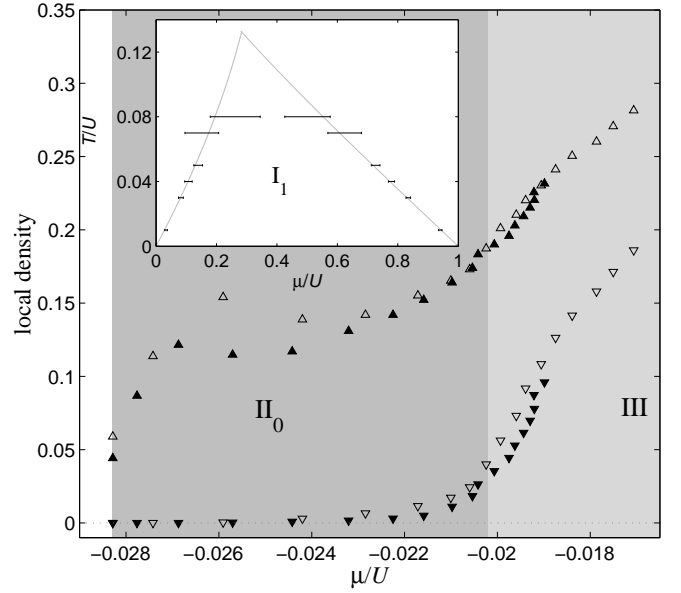


FIG. 4: **Inset:** Mott lobe I_1 for a comb lattice according to third order SCPE (solid line) and population QMC (errorbars). The latter refer to a 12×12 lattice. **Main plot:** QMC results for the on-site density of bosons on a comb lattice at $T/U = 0.01$. Upward triangles: average result for a site on the backbone. Downward triangles: average result for the farthest site from the backbone. Open and filled symbols refer to a 12×12 and a 16×16 comb lattice, respectively. The larger error on the QMC data (abscissae) is smaller than the symbol size.

bone (downward triangles) is very close to $f = 0$, and it features a sudden increase only after entering phase III . Conversely, the local density on the backbone (upward triangles) is fractional also in region II_0 , thus confirming that the superfluid is localized there.

A further confirmation of confined superfluidity is provided by the local compressibility profiles appearing in the lower panel of Fig. 3, obtained by means of QMC simulations in the case of a 12×12 comb lattice. Indeed, in the extended superfluid region the local compressibility is everywhere significantly larger than zero, whereas the curves relevant to the regions II_0 and II_1 feature a sharp decrease with increasing distance from the backbone. Note that the local compressibility within the Mott lobes I_f is everywhere zero, since, by definition, the ground state of the system can be changed only if the chemical potential μ is varied of an amount sufficient to cross the lobe border.

V. CONCLUSIONS

In summary, we reported the first analysis of the influence of topological inhomogeneity on the phase diagram of interacting bosons, considering the emblematic case of comb lattices. This supplies a basis and a con-

ceptual framework for a more general study aimed at a deeper understanding of the role of topology in quantum phase transitions. Furthermore we suggested a possible experimental setup, based on BEC arrays trapped in holographic potentials,^{10,11} where the intermediate phase occurring on a comb lattice could be observed.^{5,37,38}

The recently disclosed relation between critical behaviour and system-state entanglement⁴¹ provides a further context where the influence of geometry might play a significant role. In particular, inhomogeneous arrays have been recently proposed as quantum-information-processing devices.⁴² We point out that, owing to the formal mathematical analogy between Heisenberg and BH models (see e.g. Refs. 2 and 43), the results herewith presented have also relevant implications for quantum spin systems on inhomogeneous structures. As a concluding

remark, we observe that a comb lattice can be obtained by joining 1D structures or appropriately removing the exceeding links from a 2D regular array.⁸ This makes the structures considered here not only interesting from the theoretical point of view, but also very promising for actual realizations based on JJA technology.^{3,9,44}

Acknowledgments

The work of P.B. and A.V. has been supported by MURST project *Quantum Information and Quantum Computation on Discrete Inhomogeneous Bosonic Systems*.

-
- ¹ M. P. A. Fisher, P. B. Weichman, G. Grinstein and D. S. Fisher, Phys. Rev. B **40**, 546 (1989).
 - ² R. Fazio and H. van der Zant, Phys. Rep. **355**, 235 (2001).
 - ³ W. Kuo and C. D. Chen, Phys. Rev. Lett. **87**, 186804 (2001).
 - ⁴ D. Jaksch, C. Bruder, J. I. Cirac, C. W. Gardiner and P. Zoller, Phys. Rev. Lett. **81**, 3108 (1998).
 - ⁵ M. Greiner, O. Mandel, T. Esslinger, T. W. Hansch and I. Bloch, Nature **415**, 39 (2002).
 - ⁶ S. Sachdev, *Quantum Phase Transitions* (Cambridge University Press, Cambridge, UK) (1999).
 - ⁷ B. Douçot, M. V. Feigel'man and L. B. Ioffe, Phys. Rev. Lett. **90**, 107003 (2003).
 - ⁸ G. Giusiano, F. P. Mancini, P. Sodano and A. Trombettoni, Int. J. Mod. Phys. B **18**, 691 (2004).
 - ⁹ R. Meyer, S. E. Korshunov, C. Leemann and P. Martinoli, Phys. Rev. B **66**, 104503 (2002).
 - ¹⁰ H. Pu, L. O. Baksmaty, S. Yi and N. P. Bigelow, e-print cond-mat/0404750.
 - ¹¹ D. G. Grier, Nature **424**, 810 (2003).
 - ¹² R. Folman and J. Schmiedmayer, Nature **413**, 466 (2001).
 - ¹³ H. Ott, J. Fortagh, G. Schlotterbeck, A. Grossmann and C. Zimmermann, Phys. Rev. Lett. **87**, 230401 (2001).
 - ¹⁴ W. Hänsel, P. Hommelhoff, T. W. Hänsch and J. Reichel, Nature **413**, 498 (2001).
 - ¹⁵ R. Burioni, D. Cassi, I. Meccoli, M. Rasetti, S. Regina, P. Sodano and A. Vezzani, Europhys. Lett. **52**, 251 (2000).
 - ¹⁶ P. Buonsante, R. Burioni, D. Cassi and A. Vezzani, Phys. Rev. B **66**, 094207 (2002).
 - ¹⁷ A. Polkovnikov, S. Sachdev and S. M. Girvin, Phys. Rev. A **66**, 053607 (2002).
 - ¹⁸ V. A. Kashurnikov, N. V. Prokof'ev and B. V. Svistunov, Phys. Rev. A **66**, 031601(R) (2002).
 - ¹⁹ G. G. Batrouni, V. Rousseau, R. T. Scalettar, M. Rigol, A. Muramatsu, P. J. H. Denteneer and M. Troyer, Phys. Rev. Lett. **89**, 117203 (2002).
 - ²⁰ G. Pupillo, E. Tiesinga and C. J. Williams, Phys. Rev. A **68**, 063604 (2003).
 - ²¹ A. M. Rey, K. Burnett, R. Roth, M. Edwards, C. Williams and C. W. Clark, J. Phys. B **36**, 825–841 (2003).
 - ²² R. Roth and K. Burnett, Phys. Rev. A **68**, 023604 (2003).
 - ²³ M. Aizenman, E. H. Lieb, R. Seiringer, J. P. Solovej and J. Yngvason, Phys. Rev. A **70**, 023612 (2004).
 - ²⁴ L. Santos, M. A. Baranov, J. I. Cirac, H.-U. Everts, H. Fehrmann and M. Lewenstein, Phys. Rev. Lett. **93**, 030601 (2004).
 - ²⁵ P. Buonsante and A. Vezzani, Phys. Rev. A **70**, 033608 (2004).
 - ²⁶ P. Buonsante, V. Penna and A. Vezzani, Phys. Rev. B **70**, 184520 (2004).
 - ²⁷ F. Harari, *Graph Theory* (Addison-Wesley, Reading) (1969).
 - ²⁸ K. Sheshadri, H. R. Krishnamurthy, R. Pandit and T. V. Ramakrishnan, Europhys. Lett. **22**, 257 (1993).
 - ²⁹ L. Amico and V. Penna, Phys. Rev. B **62**, 1224 (2000).
 - ³⁰ J. K. Freericks and M. Monien, Europhys. Lett. **26**, 545–550 (1994).
 - ³¹ T. D. Kühner and H. Monien, Phys. Rev. B **58**, R14741 (1998).
 - ³² G. G. Batrouni, R. T. Scalettar and G. T. Zimanyi, Phys. Rev. Lett. **65**, 1765 (1990).
 - ³³ V. A. Kashurnikov, A. V. Krasavin and B. V. Svistunov, JETP Lett. **64**, 99 (1996).
 - ³⁴ Note that, unlike 1, the MF Hamiltonian \mathcal{H} does not conserve the number so that $\langle a \rangle = \alpha$ is not necessarily zero.
 - ³⁵ D. van Oosten, P. van der Straten and H. T. C. Stoof, Phys. Rev. A **63**, 053601 (2001).
 - ³⁶ All the calculations presented here assume periodic boundary conditions both along the backbone and the ribs of the comb lattice.
 - ³⁷ P. Pedri, L. Pitaevskii, S. Stringari, C. Fort, S. Burger, F. S. Cataliotti, P. Maddaloni, F. Minardi and M. Inguscio, Phys. Rev. Lett. **87**, 220401 (2001).
 - ³⁸ S. K. Adhikari and P. Muruganandam, Phys. Lett. A **310**, 229 (2003).
 - ³⁹ see e.g. Y. Iba, Trans. Jap. Soc. for Artificial Intelligence **16**, 279–286 (2001), e-print cond-mat/0008226.
 - ⁴⁰ M. P. Nightingale and A. Blöte, Phys. Rev. Lett. **60**, 1562 (1988).
 - ⁴¹ A. Osterloh, L. Amico, G. Falci and R. Fazio, Nature **416**, 608 (2002).
 - ⁴² P. Giorda and P. Zanardi, Phys. Rev. A **68**, 062108 (2003).
 - ⁴³ O. Rojas, E. V. Corrêa Silva, W. A. Moura-Melo, S. de Souza and M. T. Thomaz, Phys. Rev. B **67**, 115128 (2003).

(2003).

Phys. Soc. Jpn. **76**, 729 (2000).

⁴⁴ T. Yamaguchi, R. Yagi, S. Kobayashi and Y. Ootuka, J.